On the nominal transverse shear strain to characterize the severity of creasing

DOUGLAS W. COFFIN AND JOEL C. PANEK

ABSTRACT: A transverse shear strain was utilized to characterize the severity of creasing for a wide range of tooling configurations. An analytic expression of transverse shear strain, which accounts for tooling geometry, correlated well with relative crease strength and springback as determined from 90° fold tests. The experimental results show a minimum strain (elastic limit) that needs to be exceeded for the relative crease strength to be reduced. The theory predicts a maximum achievable transverse shear strain, which is further limited if the tooling clearance is negative. The elastic limit and maximum strain thus describe the range of interest for effective creasing. In this range, cross direction (CD)-creased samples were more sensitive to creasing than machine direction (MD)-creased samples, but the differences were reduced as the shear strain approached the maximum. The presented development provides the foundation for a quantitative engineering approach to creasing and folding operations.

Application: The provided equation characterizing the shear experienced by the paperboard increasing can be used to determine multiple crease tool configurations that yield the same effect on creasing (relative crease strength or springback). The range of interest in shear strain is identified for practical evaluation and further studies of creasing and folding. The differences between MD and CD creasing is further illuminated.

In order to form a defect-free and aesthetically pleasing edge on a box, Shelton [1], in an 1876 U.S. patent, specified that the paperboard first be creased and then folded such that a smooth and straight inner bead developed along the inside edge. In a 1912 U.S. patent, Bird [2] illustrated the importance of delamination to the creased zone. These two aspects, (1) forming the crease geometry and (2) preparing the paper for ease of delamination, are essential for a successful creasing operation. A recent literature review pertaining to creasing and folding [3] concluded that using a measure of a nominal transverse shear-strain induced during creasing would be fruitful to characterize the behavior of a paperboard under various creasing tool geometries. In fact, as early as 1939, Halladay and Ulm [4] captured this concept with what they termed "angle of break". Nagasawa et al. [5,6] defined a shear strain measure for a rounded rule and characterized various aspects of creased board such as folding resistance, tensile strength, and the presence of cracks. Coffin and Nygårds [3] followed the same reasoning of reference [5] and presented a transverse shear strain equation valid for a square-tipped rule. Coffin and Panek [7] presented a more general measure for shear strain for generic rules and channels with rounded corners. The latter expression allows one to characterize the effects of tooling that span the spectrum from fully rounded rules to square-tipped rules. The objective of the following study is to establish that the transverse shear equation, presented by Coffin and Panek [7], provides a robust measure that can normalize creasing data for a wide range of tool geometries.

THEORY

Figure 1 provides the geometry for a generic creasing operation. Note, that the penetration, p, is the maximum distance the tip of the rule travels relative to the top surface of the channel. The crease depth, z, is the penetration plus the board thickness, h. The uncreased sample corresponds with $z=0$ or $p=-h$. The lines on the creased material shown in Fig. 1 illustrate a permissible deformation the board might undergo during the creasing. For the undeformed paperboard, the lines formed a square gird, and the deformation shown results from simple transverse shearing of the paperboard. In other words, z direction (ZD) compression and machine direction (MD) or cross direction (CD) (in-plane) elongation are ignored. This assumption attributes all the deformation to direct transverse shear and is approximately correct as borne out by inspection of micrographs presented by Coffin and Nygårds [3] and Halladay and Ulm [4]. The measure of shear, γ, is defined as the change in angle of the originally square lines as illustrated in the insert of Fig. 1.

With the assumptions outlined above, the angle, θ, that forms in the free-span region is derived in the Appendix and the final expression is written as:

$$\tan(\theta) = \frac{\sqrt{(1-\kappa)^2+\lambda(2+\lambda)}-(1-\kappa)(1+\lambda)}{\lambda(2+\lambda)},$$

$$\text{which} = \frac{\kappa(2-\kappa)}{2(1-\kappa)} \text{ for } \lambda = 0 \tag{1}$$

where $\kappa=z/(r_c+r_r+t)$ and $\lambda=\frac{(c-b-2t)}{2(r_c+r_r+t)}$ are the dimensionless

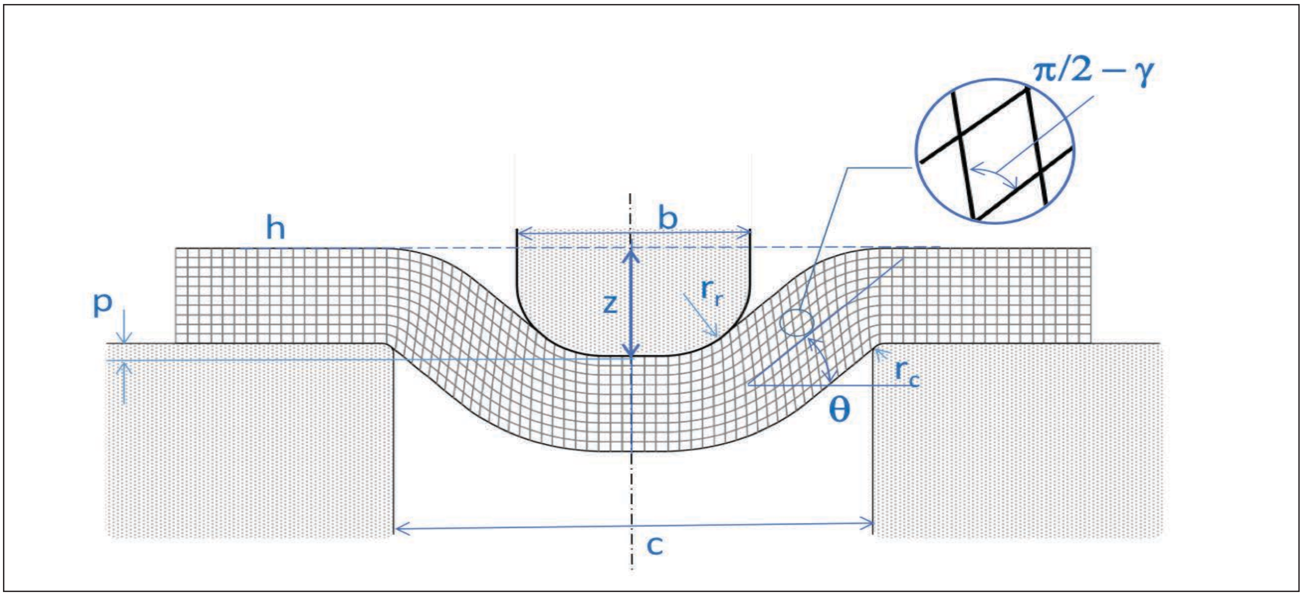

1. Crease geometry.

crease displacement and crease clearance, respectively. The shear strain in the free-span region is then determined as:

$$\tan(\gamma) = \theta = tan^{-1}\left(\frac{\sqrt{(1-\kappa)^2+\lambda(2+\lambda)}-(1-\kappa)(1+\lambda)}{\lambda(2+\lambda)}\right) \quad (2)$$

Eq. 1 and Eq. 2 reveal that this shear measure is only a function of two dimensionless parameters, κ and λ. The crease-clearance, λ, is significant because it determines the free-span of the paper between the rule and the channel. Note that the dimensionless parameters only depend on the sum of the tooling radii and the caliper. Increasing this sum decreases λ and κ and the resulting shear strain, γ.

For the case of no clearance, λ=0 (second part of Eq. 1), there is a maximum depth of draw at which point θ=90°. After this point, the paperboard will be drawn (or extended) in to the tooling, but the extent of shear remains the same. The maximum value of the shear, γ_{max} = 57.20°, is when λ=0 and κ =1.

For the case where the clearance is less than zero, λ<0, there is a maximum depth of draw, where further creasing must be accompanied with a compression of the thickness. Using just shearing strain to characterize the severity of the crease beyond this point is not justified. This critical draw occurs when the quantity within the square-root symbol of Eq. 1 is zero. That translates to:

$$z_{cr} = (r_c + r_r + t)\left(1 - \sqrt{|\lambda|(2+\lambda)}\right) \quad (3)$$
$$\tan(\gamma_{cr}) = sin^{-1}(1+\lambda)$$

If the rule and channel radii approach zero and the corners are sharp, a nominal shear strain could be expressed simply as previously stated in [3] as:

$$\tan(\gamma_{square}) = \frac{2z}{c-b} \quad (4)$$

For the case where the rule radius is half the rule width and the channel radius approaches zero, the shear strain could be expressed as previously given in [5] as:

$$\tan(\gamma_{rounded}) = \frac{2z}{c} \quad (5)$$

Eqs. 4 and 5 represent alternative representations of the shear strain compared to Eq. 2. The curves of **Fig. 2** provide comparisons of these predictions for three cases: (a) λ>0, (b) λ=0, and (c) λ<0. For small depth of draws, Eq. 2 reasonably matches both Eqs. 4 and 5. The match is best for the case of λ>0, but as the creasing operating parameters produce more severe shearing deformation, the various shear measures deviate. The advantage of Eq. 2 over Eqs. 5 and 6 is that it applies to a full range of tool geometries. In addition, Eq. 2 highlights that for the case of $\lambda \leq 0$, maximum shear strain occurs for a finite draw, and further creasing beyond this point would introduce ZD compression and possibly MD-CD extension. The advantage of Eqs. 5 and 6 are that they are simpler and provide a measure for all values of crease draw.

METHODS & MATERIALS

A series of creasing and folding tests were completed on a commercially produced coated solid bleached sulfate (SBS) board (309 g/m²; h=0.401 mm; TAPPI Standard Test Methods T 410 "Grammage of paper and paperboard [weight per unit area]" and T 411 "Thickness [caliper] of paper, paperboard, and combined board," respectively).

Paperboard samples were creased with a custom laboratory creasing device. The channel segment was mounted to the base structure and the rule segment was mounted to a

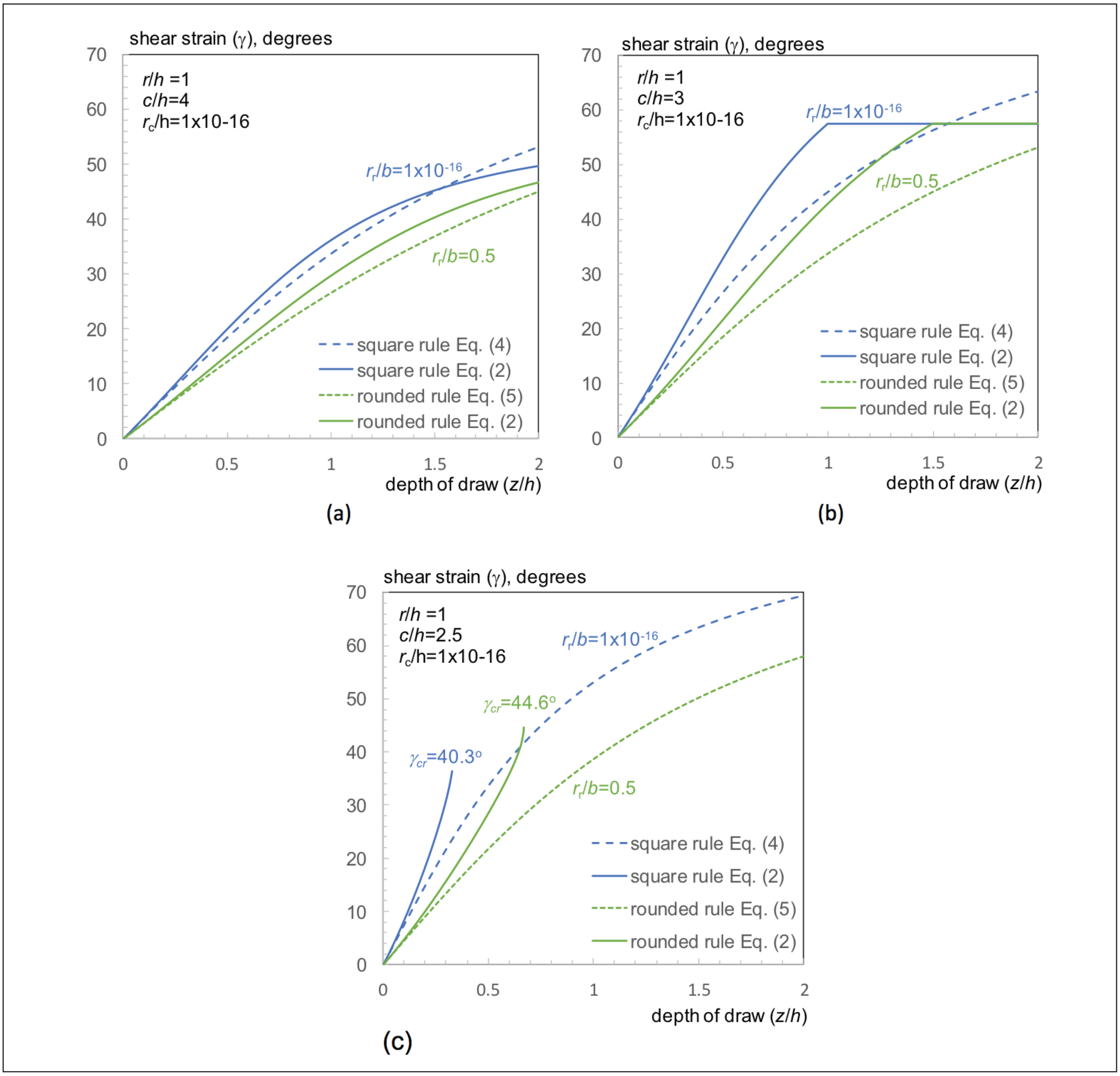

2. Comparison of shear values from Eqs. 2, 5, and 6 for example cases of (a) $\lambda>0$, (b) $\lambda=0$, and (c) $\lambda<0$.

linear motor. The linear motor controlled the motion of the rule to a target penetration depth, p, (+/- 0.005 mm) as reported in **Table I**. The velocity of the rule tip was 160 mm/s at point of contact with the paperboard. At this velocity, the total contact time of the rule with the paperboard was ~10 ms.

The tool segments (14 mm x 20 mm x 85 mm) are made of hardened steel, with a dimension tolerance of +/-0.02 mm. For the tooling used in this study, the rule width, b, and channel width, c, are given in Table I. The rules (A-F) were 50.8 mm long and 1.5 mm high, with either a flat tip profile having a 45° chamfered edge (A-F) or a rounded tip (G and H). The channels were 51.4 mm long and 1.0 mm deep with a 45° chamfered edge. Table I also provides a sketch of the crease at maximum penetration for each set of tooling geometry, as well as the dimensionless clearance and crease depth.

Paperboard samples (100 mm x 300 mm) were clamped on the narrow ends, with one clamp fixed to the base and the other clamp mounted on a slide. The sample was held under a tension of 1.1 kN/m using weights (11 kg) attached to the slide clamp. The rule and channel were oriented so that they were parallel to the short dimension of the sample. In this configuration, the applied tension is perpendicular to the crease. Strips were creased in both the MD and the CD and aligned with the creasing tools. Creases where the axis was aligned in the MD of the paperboard were designated as MD creases, and creases aligned in the CD of the paperboard were designated as CD creases. Four creases were produced on

Set	Crease Shape at Maximum Penetration	Tooling Geometry, mm	Range of Penetration Depths (p), mm	Crease Clearance (λ)	Range of Crease Depth (κ)
A	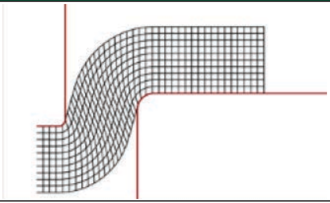	b= 0.35, c = 1.23 r_r = 0.04, r_c = 0.1	0.00 to 0.20	0.074	0.74 to 1.11
B	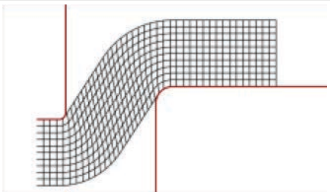	b= 0.35, c = 1.44 r_r = 0.04, r_c = 0.1	0.00 to 0.20	0.269	0.74 to 1.11
C	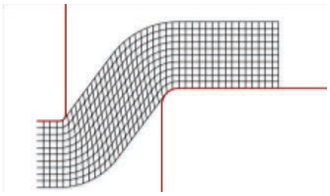	b= 0.35, c = 1.51 r_r = 0.04, r_c = 0.1	0.00 to 0.20	0.333	0.74 to 1.11
D	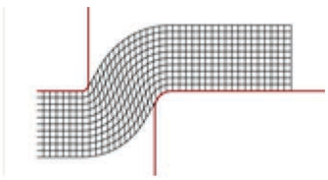	b= 0.63, c = 1.44 r_r = 0.04, r_c = 0.1	-0.15 to 0.00	0.009	0.46 to 0.73
E	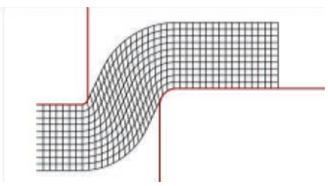	b= 0.63, c = 1.51 r_r = 0.04, r_c = 0.1	-0.10 to 0.10	0.074	0.56 to 0.93
F	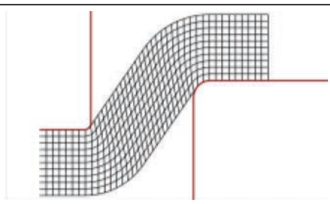	b= 0.63, c = 1.89 r_r = 0.04, r_c = 0.1	0.00 to 0.30	0.426	0.74 to 1.25
G	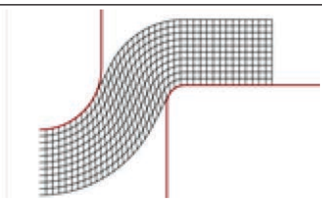	b= 0.70, c = 1.24 r_r = 0.35, r_c = 0.1	-0.24 to 0.25	-0.153	0.30 to 1.31
H	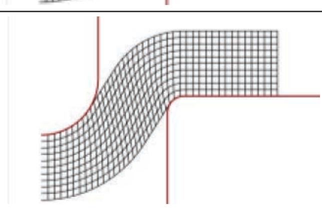	b= 0.70, c = 1.35 r_r = 0.35, r_c = 0.1	-0.26 to 0.24	-0.088	0.13 to 1.13

I. Creasing settings.

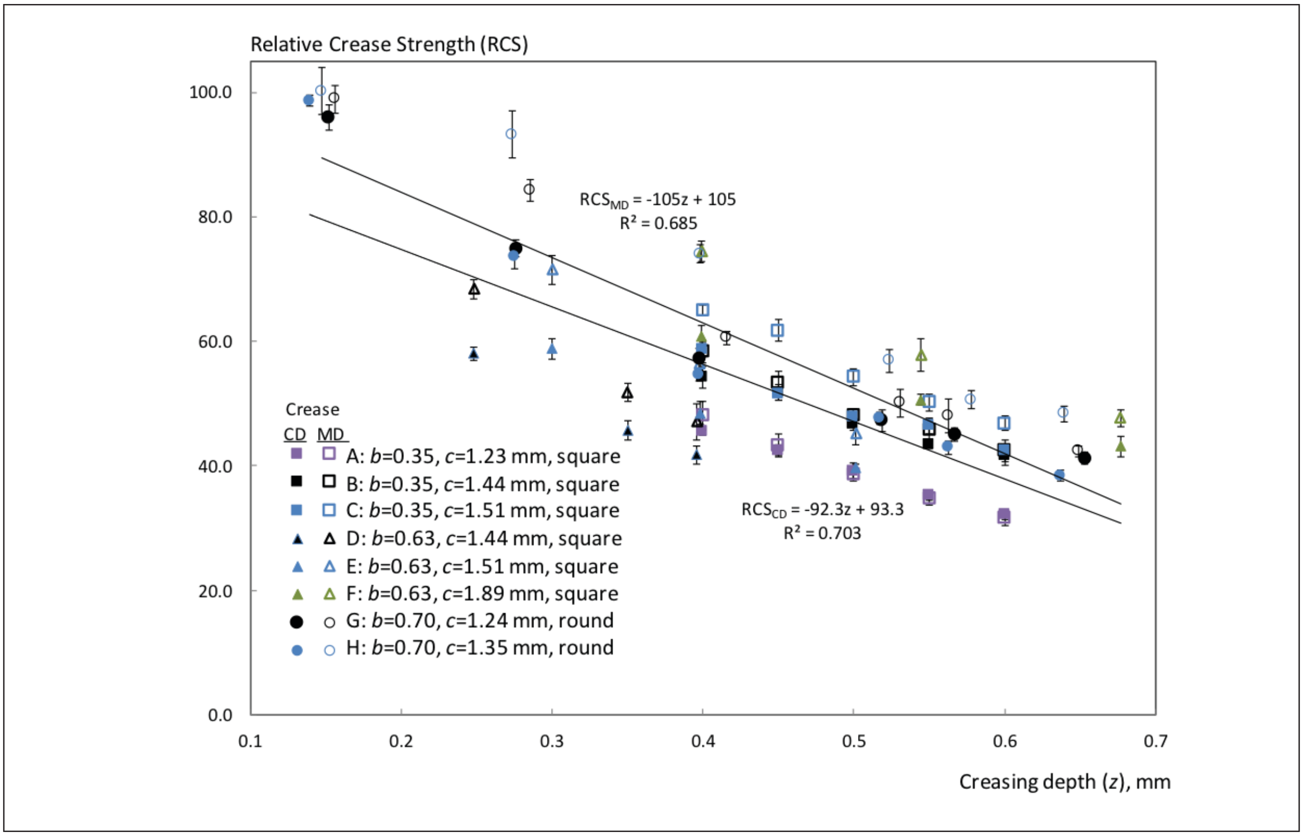

3. Relative crease strength (RCS) versus depth of crease.

each strip and evenly spaced along the longer direction of the sample. Samples were then cut to provide one crease per specimen. The height and width of each crease was measured.

The creased specimens were folded to 90° using a Lorentzen & Wettre (Kista, Sweden) bending tester, code 160. Test pieces were 38-mm wide, the bending length was 10 mm, and the crease was aligned to within 1.0 mm of the clamp. The sample was folded to 90° (45°/s) and then back to 0°. The bending moment [mNm] versus angle of bend was recorded for the full curve. Eight replicates were measured for each case given in Table I.

The relative crease strength (RCS) was calculated as the ratio of the uncreased peak moment divided by the creased peak moment, using the peak bending moments less than an angle of 30°. The springback ratio was calculated as the ratio of the uncreased peak moment divided by the creased peak moment, using the bending moments at 90° after 15 s of relaxation.

RESULTS

The testing produced sets of data for eight different creasing-tool configurations and up to six penetration depths, in both MD and CD. The shear strains for each creasing configuration were calculated using Eqs. 1 and 2. **Figures 3** and **4** provide respective graphs of RCS versus penetration depth and shear strain for each tooling set. In general, Fig. 3 demonstrates that as crease penetration increased, the RCS decreased, but each tooling configuration resulted in a unique curve. When RCS was plotted against shear strain, Fig. 4, the curves converged to produce one MD and one CD curve. The linear lines demonstrate the improvement gained by describing RCS as a function of shear strain (R^2>0.95) instead of crease depth, and the red-lines suggest the diminishing effect of creasing on RCS for low creasing angles. Below a shear strain of approximately 10°, the creasing had negligible effect on RCS, but as shear strain increased, RCS decreased. The CD crease required a higher peak moment (33% increase on average) than an MD crease for all levels of creasing. As indicated in Fig. 4, the CD crease showed a larger drop in RCS for intermediate levels of strain, but the difference diminished as the shear-strain increased.

Springback ratio versus shear strain, **Fig. 5**, shows that the various tooling configurations formed unique MD and CD curves. The bi-linearity of the CD curve is more pronounced for springback compared to RCS. This suggests that the response to folding for this paperboard is most sensitive for CD creasing between 10° and 20° shear strain.

Strong linear correlations were found between measured MD and CD properties, as indicated in **Table II**. Only the crease width was independent of crease direction, and as one would expect, slightly larger and strongly correlated to channel width (width =1.025 c, R^2=0.88). The crease height for CD creases was on average 79% of the height for MD creases, while the RCS for a CD crease was on average 90% that of an MD crease. Note that the intercept of the correlation of MD and CD

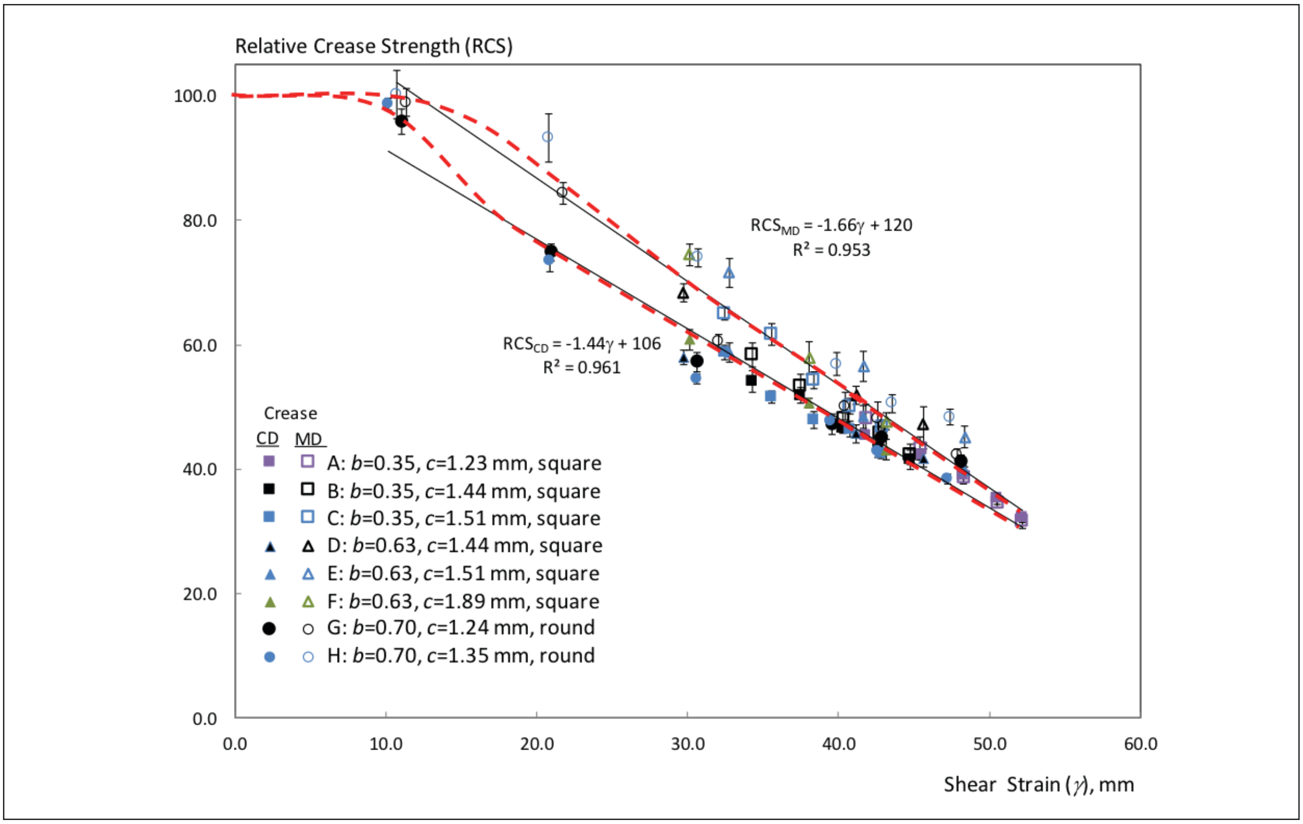

4. RCS versus transverse shear strain. Error bars are 95% confidence limits of mean.

Property	Slope CD vs. MD	Intercept	Coefficient of Determination, R^2
Crease width	0.989	0.008	0.980
Crease height	0.760	0.003	0.981
RCS	0.836	3.57	0.917
RCS, γ>20°	0.679	11.53	0.921

II. Correlations between machine direction (MD) and cross direction (CD) measured crease characteristics (RCS = relative crease strength).

RCS does not pass through zero, reflecting a more complex response of RCS to creasing as demonstrated in Fig. 4.

Figure 6 shows the bending moment versus bending angle for select creasing configurations. These represent average curves that were normalized to the peak moment (less than 30°) of the uncreased sample yielding that the peaks in the curves are RCS values. The shear values given to three significant figures were calculated for the respective curve. The shear values reported to two significant figures are a nominal value for the group of similarly colored curves. The solid lines are for the square-tipped rules, and the dashed lines are for the rounded rules.

DISCUSSION

The convergence of the data into MD and CD curves (Figs. 4 and 5) demonstrates that the transverse shear strain (Eq. 2) is a meaningful measure to characterize crease severity for a wide range of tooling configurations. This validates the hypothesis that transverse shear dominates creasing and that a nominal measure of the shear strain provides a means to quantify creasing behavior. For the paperboard tested, RCS versus shear strain was linear in the range of strain from 20° to 55°. Therefore, only two calibration points are needed to apply Eqs. 1 and 2 to determine a range of tooling parameters that yield the same shear strain and thus the same RCS.

Creasing at shear strains less than 10° did not appear to decrease the force required to fold the board. The peak moment in an uncreased board marks the onset where the bending initiates a delamination and buckling of the inner plies and the start of an uncontrolled bead formation. Once the creasing creates enough shear damage, the delamination initiates at lower load and the crease shape provides for a controlled bead formation, which manifests in a reduction of peak moment. Figures 4 and 6 show that for shear angles near 10°, the RCS is close to 100%, and the bending moment versus angle curves are quite similar to the uncreased samples, indicating that the creasing operation at this level was essentially an elastic deformation.

Because a CD crease engages the MD properties, the response should be more brittle in nature (more damage at

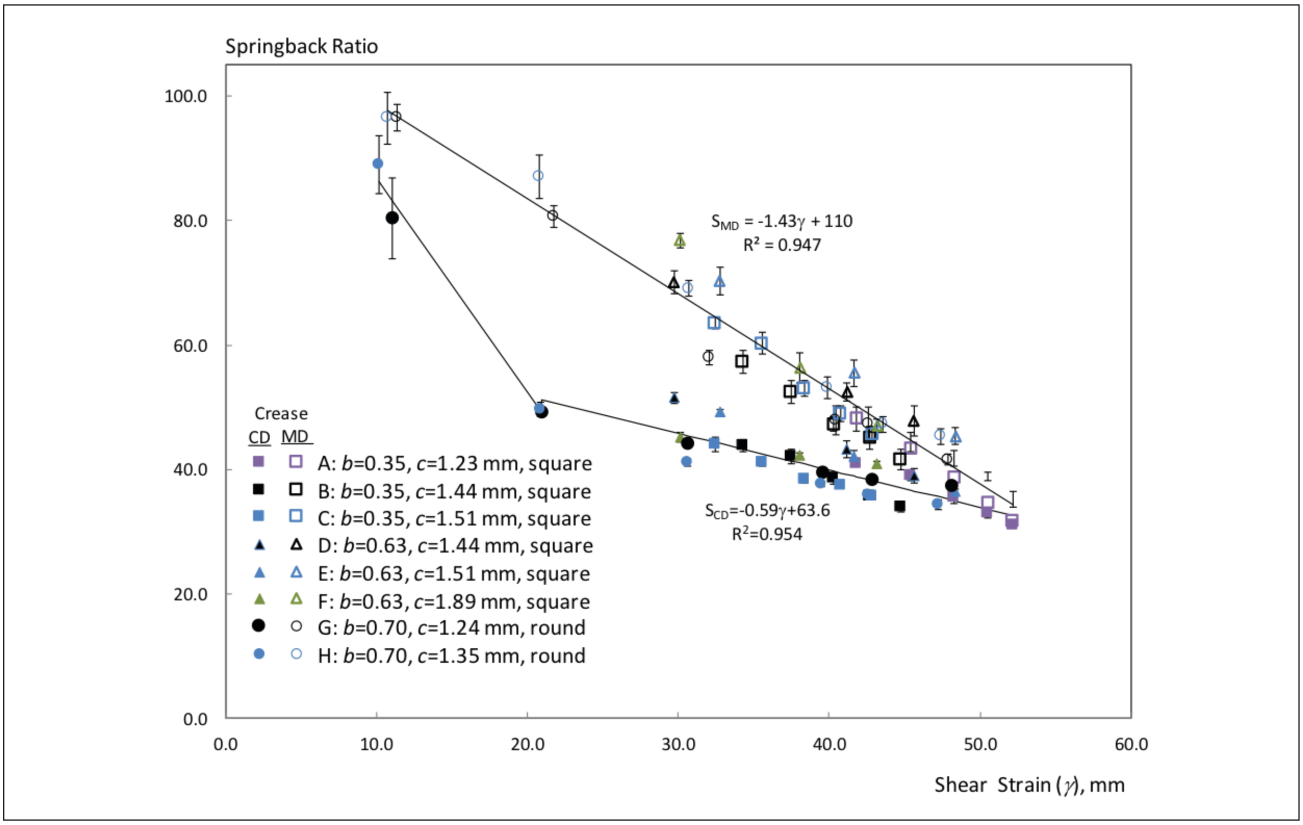

5. Springback ratio versus transverse shear strain. Error bars are 95% confidence limits of mean.

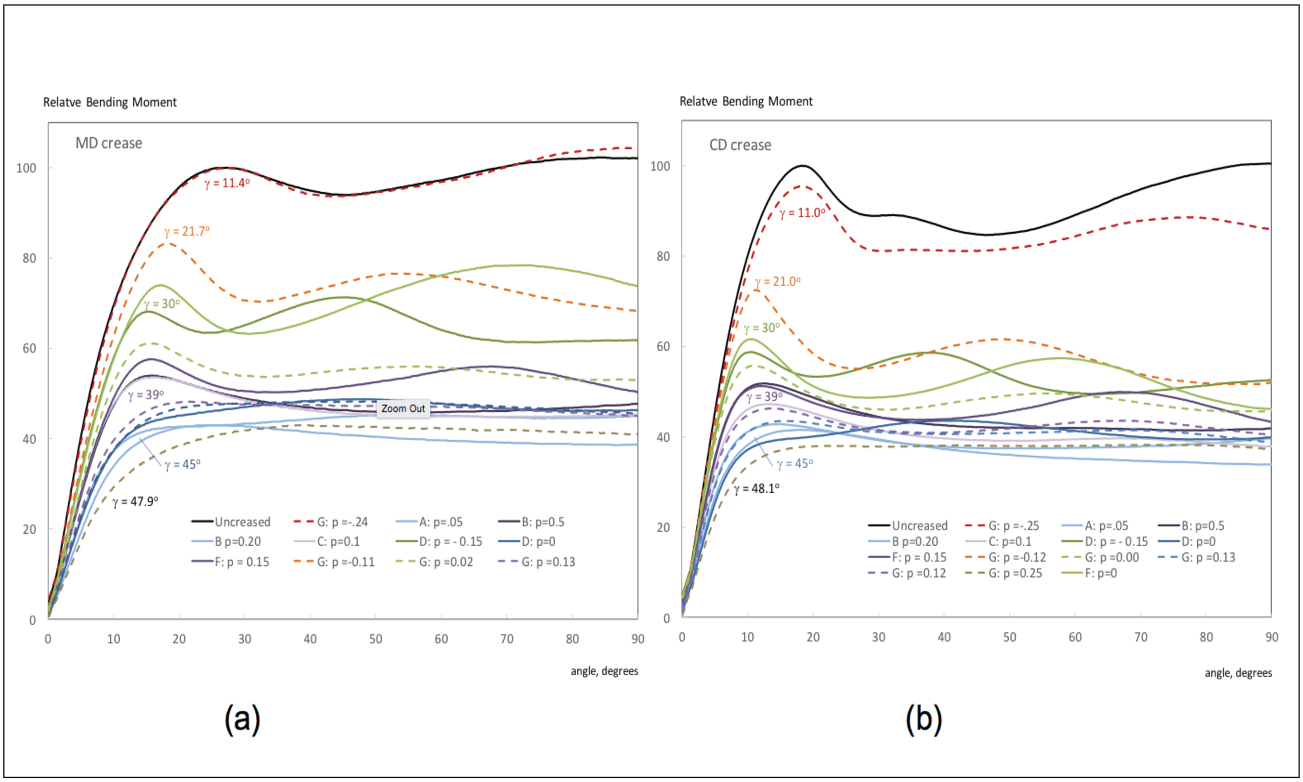

6. Sample moment versus angle of bend for (a) machine direction (MD) creases and (b) cross direction (CD) creases.

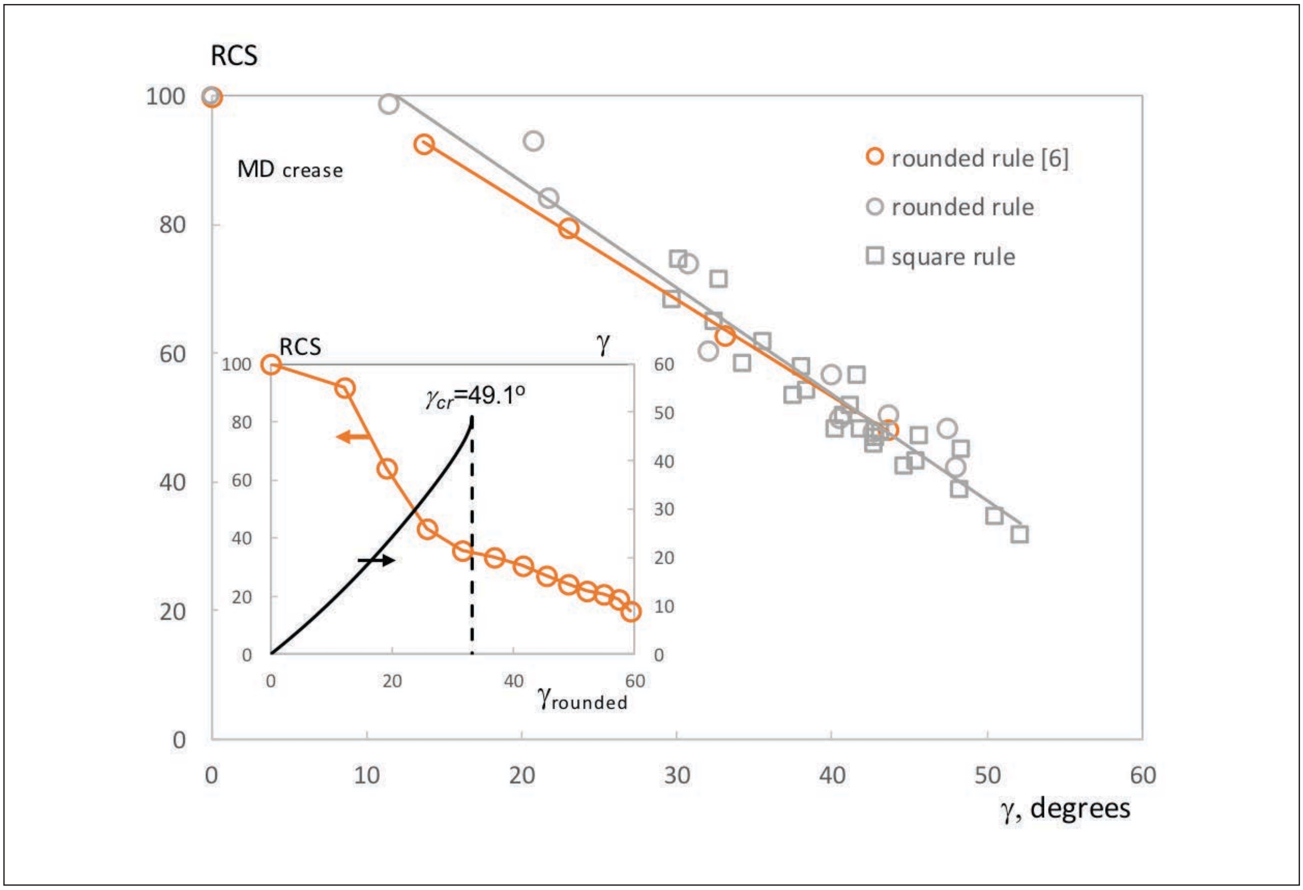

7. Comparison to results in literature [6].

lower strains) compared to MD creases. This is observed in the greater reduction of both RCS and springback ratio in the range of 10° to 20° shear strain. In addition, the bending moment versus angle curves of Fig. 6 exhibit a sharper decrease in post-peak response. The major reduction in springback ratio for a CD creased sample indicates more severe damage from creasing. The lower CD crease height compared to the MD crease height for the same strain suggests more plastic flow for the MD crease, yet the relative decrease in strength is lower, suggesting that the plastic deformation in an MD crease does not improve the ability to delaminate in folding compared to the CD crease.

The theory predicted a maximum shear angle of γ_{max} = 57.20°, beyond which shear would be constant. In Fig. 4, the MD and CD curves intersect at γ = 63.6°, and in Fig. 5 the intersection is at γ = 55.2°. This gives an average of γ = 59.4°. Therefore, at the maximum strain, the relative change in MD and CD are the same and the shear strain has reached a maximum level. For the paperboard tested, the RCS is less than 30% in this region and below desired levels sought in practice.

Figure 7 compares the current MD crease data along with that from [6], plotted against γ, but only up to the critical strain (γ=49.1°, because clearance was negative [6]). Figure 7 shows that both sets of data produced essentially the same RCS versus strain curve. Greater creasing depths were evaluated in [6] beyond the range of validity of Eq. 2. Therefore, Eq. 5 was used to plot the RCS data from [6], as shown in the inset graph of Fig. 7. The equivalent shear strain, γ, is also shown on the secondary ordinate up to the critical strain. This graph reveals that after the critical strain, the slope of the RCS curve is greatly reduced. This is presumably because the shear strain remains almost constant, but additional ZD compression and CD tension are added. This further suggests that RCS is mainly controlled by the extent of transverse shear deformation created in the creasing operation. The region of interest for practical creasing operations should be in the range of 20° to 50°, and the data in the inset Fig. 7, which represents creasing past the critical shear, is in a regime beyond typical industrial practice.

CONCLUSIONS

A two-parameter transverse shear measurement, Eq. 2, was shown to provide a robust characterization of creasing severity. By including corner radii of the tooling, the expression is applicable to a wide range of configurations and can provide more guidance than current industrial strategies. The equation predicts that the magnitude of the transverse shear strain reaches a maximum of 57.2°, which is further reduced for cases of negative clearance. Ninety-degree fold tests showed that the relative crease strength and springback correlated well with the transverse shear strain. For a given paperboard, minimal tests could be completed to determine the shear strains that reduce the relative crease strength to the desired level (say 60%), and Eq. 2 can be used subsequently to determine a family of tooling geometries that will produce the desired reduction.

The folding tests revealed that initial creasing penetrations are elastic; followed by an inelastic region where damage reduces peak bending moment. The CD creased samples were more sensitive to creasing in the mid-range of shear strains (10°–20°), but as the shear strain approached the maximum, the differences in relative crease strength for MD and CD creased samples was negligible. Comparison to creasing data from the literature showed that the CD creased behavior of two papers was essentially the same, and that creasing beyond the critical strain denoted a decrease in the effectiveness of the creasing.

The presented approach to creasing offers a quantitative engineering-based approach to creasing and folding that should allow industry to move beyond the current practice of applying heuristic guidelines. **TJ**

LITERATURE CITED

1. Shelton, E. De. F., U.S. pat. 183423 (Oct. 17, 1876).
2. Bird, C.S., U.S. pat. 1,022,923 (April 9, 1912).
3. Coffin, D.W. and Nygårds, M., "Creasing and folding of paper," *Trans. Fundam. Res. Symp., 16th,* 69: 136(2017).
4. Halladay, J.F. and Ulm, R.W.K., "Creasing and bending of folding boxboard," *Pap. Trade J., Tappi Section*, 108(5): 36(Feb. 2., 1939).
5. Nagasawa, S., Fukuzawa, Y., Yamaguchi, D., et al., "Deformation characteristics of creasing on paperboard under shallow indentation," *Adv. Fract. Res., Proc. Int. Conf. Fract., 10th*, ICF10-0202OR, Elsevier Science, New York, 2001.
6. Nagasawa, S., Fukuzawa, Y., Yamaguchi, D., et al., *J. Mater. Process. Technol.* 140(1-3): 157(2003).
7. Coffin, D.W. and Panek, J.C., in *Progress in Paper Physics Seminar 2016 Conference Proceedings* (S. Schabel and H.-J. Schaffrath, Eds.), Technische Universität Darmstadt, Darmstadt, Germany, 2016, p. 132.

APPENDIX

Consider a Cartesian coordinate system (X,Y) with origin aligned with the center of the rule and the top surface of the channel. The position vector for any point (X,Y) located in

ABOUT THE AUTHORS

Several years ago, we began working on creasing and folding issues, starting with a critical review of the literature and then examining the mechanics of creasing and folding. There appeared to be a gap in the literature dealing with how to characterize the severity of creasing in terms of some fundamental measure of shear. The authors then sought to develop a robust measure that can normalize creasing data for a wide range of tool geometries.

The research here complements prior work using shear strain expressions to characterize the behavior of a paperboard under various creasing tool geometries. It adds a more robust equation that is valid over a range of realistic results. This research extends previous literature in terms of using a transverse shear measurement to characterize creasing severity. The new expression accounts for tooling geometry and multiple data sets collapsed to the same curve.

Although we initially set up the model and developed expressions rather quickly, it took time and retrospection to realize we needed to invert the expressions to make them usable and choose the best expression for shear strain. Once we did this, everything seemed to fall into place, but it did take discipline to stick with the research over a period of years.

Rediscovering the 19th century patents and the work of Halladay and Ulm from 1939 provided new perspectives and insights that are missing from more recent literature. A most interesting aspect was the development of a critical shear strain and how one can interpret previous data in light of this knowledge (Fig. 7).

Coffin

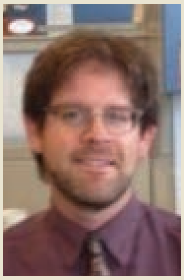

Panek

Those that produce paperboard, convert it, or design packaging can use the shear measurement as an indication of creasability. This can help tie relative crease strength to board properties and tooling geometry. Results from one set of tooling can be transferred to different tooling. This research also provides knowledge that can shift the way people working in the field look at creasing and folding. The next step is to apply the approach in practical situations. Also, there is an operating window for the creasing operation that will lead to successful creasing and folding for a given paperboard, and we need to better define that window for converters.

Coffin is professor in the Department of Chemical, Paper, and Biomedical Engineering at Miami University in Oxford, OH, USA. Panek is research scientist with WestRock in Richmond, VA, USA. Email Coffin at coffindw@miamioh.edu.

the free-span region is made of up three components: the flat portion of the rule, the arc of the wrap around the rule radius, and the angle (θ) free span section. This position vector $\hat{R}$ can be written as:

$$\begin{aligned}\hat{R}(X,Y) = &\left[\frac{b}{2} - r_r + (r_r + h - Y)\sin(\theta) + \left(X - \frac{b}{2} + r_r - (r_r + h - Y)\theta\right)\cos(\theta)\right]\hat{\imath} \\ &+ \Big[-z - h + Y + (r_r + h - Y)(1 - \cos(\theta)) \\ &+ \left(X - \frac{b}{2} + r_r - (r_r + h - Y)\theta\right)\sin(\theta)\Big]\hat{\jmath}\end{aligned}$$

Assuming that lines of constant Y remain parallel and maintain the same spacing such that the thickness, h, is preserved (as shown in Fig. 1), then the deformation can be described as the change in the unit vectors ($\hat{i}, \hat{j}$), which formed a right angle on the undeformed material: $\frac{\pi}{2} - \gamma$. The magnitude of these two vectors can be written as stretches (Λ_1, Λ_2), which equal:

$$\Lambda_1 = \left\|\partial\hat{R}(X,Y)/\partial X\right\| = 1 \text{ and } \Lambda_2 = \left\|\partial\,\hat{R}(X,Y)/\partial Y\right\| = 1 + \theta^2$$

The dot product of the two partial derivatives of the position vector yields:

$$\Lambda_1\,\Lambda_2\cos\left(\frac{\pi}{2} - \gamma\right) = \sqrt{1+\theta^2}\,\sin(\gamma) = \partial\hat{R}(X,Y)/\partial X \cdot \partial\hat{R}(X,Y)/\partial Y = \theta$$

This expression is equivalent to:

$$\tan(\gamma) = \theta$$

For completeness, the stretches indicate inextensibility along the length of the paper, and a stretch through the thickness to maintain constant thickness, h. This is analogous to a case of direct shear.